

Generation of sub-3 fs pulses in the deep ultraviolet

Florentin Reiter,^{1,2} Ulrich Graf,¹ Martin Schultze,^{1,3} Wolfgang Schweinberger,¹ Hartmut Schröder,¹
 Nicholas Karpowicz,¹ Abdallah Mohammed Azzeeer,⁴ Reinhard Kienberger,^{1,2}
 Ferenc Krausz,^{1,3} and Eleftherios Goulielmakis^{1,*}

¹Max-Planck-Institut für Quantenoptik, Hans-Kopfermann-Strasse 1, D-85748 Garching, Germany

²Physik Department, Technische Universität München, James Franck Strasse, D-85748 Garching, Germany

³Department für Physik, Ludwig-Maximilians-Universität, Am Coulombwall 1, D-85748 Garching, Germany

⁴Physics and Astronomy Department, King Saud University, Riyadh, 11451, Kingdom of Saudi Arabia

*Corresponding author: elgo@mpq.mpg.de

Received April 14, 2010; accepted May 11, 2010;
 posted June 11, 2010 (Doc. ID 126799); published June 28, 2010

We demonstrate generation and measurement of intense deep-ultraviolet light pulses with a duration of ~ 2.8 fs (FWHM of the intensity envelope) and a wavelength distribution between 230 and 290 nm. They emerge via direct frequency upconversion of sub-4 fs laser pulses of a carrier wavelength of ~ 750 nm focused into a Ne-filled, quasi-static gas cell. Dispersion-free, third-order autocorrelation measurements provide access to their temporal intensity profile. © 2010 Optical Society of America

OCIS codes: 190.7110, 190.7220, 320.5550.

Development of ever-shorter laser pulses provides time-resolved spectroscopy with ever-higher resolution to explore and control dynamics in the microcosm. Attosecond technology [1] has recently advanced this resolution to the atomic unit of time [2], and via its key tools, attosecond extreme ultraviolet (XUV) pulses and controlled few-cycle near-IR (NIR) laser fields, have allowed insight into and control of electronic processes in atoms [3] and in molecules [4]. For triggering and steering of ultrafast electron dynamics in the valence shell of molecules, solids, nanoparticles, and clusters, few-cycle light pulses in the deep and vacuum UV (DUV/VUS, 100–300 nm) should be added to the toolbox of modern ultrafast and attosecond science [5,6].

Generation of ultrashort UV pulses with durations ranging from ~ 100 fs to the few-cycle regime is now possible by use of several techniques. Nonlinear pulse broadening and compression [7,8], four-wave-mixing in hollow-core fibers [9] or in filaments [10] and direct frequency upconversion of multicycle [11,12] or few-cycle pulses in the NIR [13,14] are the most prominent examples. The latter technique has permitted generation of, hitherto, the shortest pulses in the deep UV (~ 3.7 fs and ~ 4.5 eV) characterized with FROG [14], and has indicated the potential for further reduction of their duration when driven by shorter NIR pulses.

Here we explore this potential by direct frequency upconversion of sub-4 fs NIR pulses into the deep UV. To overcome the limitations imposed by the dispersion of nonlinear solid-state detectors, we have opted for an approach combining an all-reflective autocorrelation [15] and a gas-phase nonlinear medium (Kr). Such a scheme has been employed successfully for the characterization of attosecond pulse trains in the VUV/XUV regime [16–18].

Figure 1 illustrates the schematic of the experimental apparatus. Sub-4 fs pulses [2,19] at a carrier wavelength of 750 nm and an energy of 0.25 mJ are focused by a concave ($f = 600$ mm) silver-coated mirror into a 3-nm-long quasi-static gas cell filled with neon (~ 5 bar) to produce the third harmonic of the broadband fundamental radiation. The cell is assembled in a vacuum chamber. The

background pressure is maintained at 10^{-1} mbar. The energy of the emerging deep UV pulses is approximately $1.5 \mu\text{J}$ at the source [14]. Filtering the UV pulses out of their intense fundamental is accomplished by a pair of Brewster reflections (74° at 750 nm) from silicon mirrors installed in a second vacuum chamber, 1 m downstream from the source. The s -polarized component of the NIR pulses, which is relatively weak with respect to the p -polarized component ($s:p$ ratio $\sim 10^{-3}$) but comparable to the UV radiation, is suppressed prior to the NIR-to-UV conversion by passage through a series of (15) thin $2 \mu\text{m}$ polymer pellicles installed at the Brewster angle. The two filtering schemes allow NIR pulse suppression down to ~ 50 nJ and shift their central energy to ~ 2 eV (622 nm) due to the spectrally nonuniform reflectivity of the silicon mirrors. The energy of the transmitted UV pulses is 300 nJ. An aperture installed in the beam path could further suppress the more diverging, when compared to the UV, fundamental.

Dispersion-free beam splitting of the UV beam is implemented by a module of two D-shaped, plain aluminum mirrors, one of which is mounted on a translation stage controlled with a piezo actuator with nanometric accuracy. The two beams of comparable intensity are then focused by an $f = 125$ mm, superpolished, aluminum-coated mirror to ionize krypton atoms ($\sim 10^{-7}$ mbar) at the entrance of a high-resolution reflectron-type ion-mass

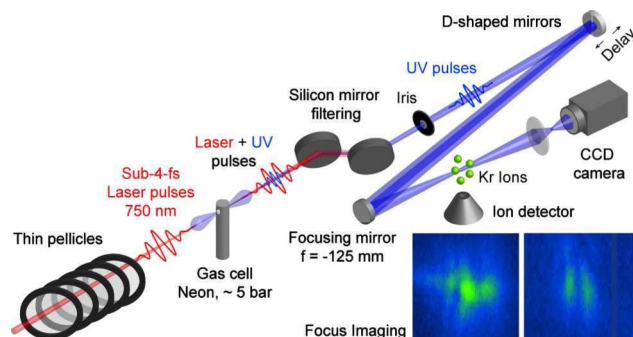


Fig. 1. (Color online) Experimental setup for the generation and characterization of sub-3 fs pulses in the deep UV.

spectrometer. To ensure optimal spatial as well as temporal overlap of the two beams in the focus, a telescope is used to image the focal plane onto a detector, based on a phosphor screen and a CCD camera. Representative interference snapshots of the UV beams at the focal plane are shown at the lower right corner of Fig. 1.

Three-photon ionization of Kr atoms (ionization potential: $I_p = 13.99$ eV) by our broadband UV pulses, spanning over a band of more than 1 eV in photon energy and centered at ~ 4.7 eV [Fig. 2(a)], is the nonlinear process of choice for the autocorrelation scheme presented. The suitability of krypton as a gas-phase nonlinear medium has been demonstrated earlier [20] for pulses in the vacuum UV range. To ensure that the complex electronic-level structure of Kr, near the ionization threshold, does not affect its nonlinear properties when broadband pulses are used to ionize and partially populate these levels, we first set out to determine the nonlinearity of the ionization yield under our experimental conditions. Figure 2(b) shows the variation of the Kr^+ yield versus energy of the UV pulses (estimated intensity in the focus: $I_{\text{UV}} \sim 1\text{--}2 \cdot 10^{13}$ W/cm², pulse energy after all optical elements and aperture ~ 20 nJ), which is varied by tuning the pressure of neon in the generation cell. A slope of ~ 2.9 , derived by the fitting of these data, is compatible with the anticipated third-order nonlinearity. Similar results are obtained when the intensity of the UV pulses is varied by an aperture. The variation of the Kr^+ yield as a function of the delay (step 0.1 fs) between the two UV pulse replicas in the focus is shown in Fig. 3(a) (square dots) and corresponds to a third-order fringe-resolved autocorrelation trace of the UV pulses. The interference fringes across the recorded trace are compatible with a central energy of ~ 4.7 eV (263 nm), in agreement with that inferred from the spectrum shown in Fig. 2(a). A slower beating at the frequency of the residual laser that survives filtering is also discernible, particularly at positive delays.

We derive the duration of the UV pulses utilizing two complementary approaches. Before doing so, we comment on the presence of interference fringes—at the frequency of the laser—and their filtering. As the intensity of the laser pulses in the focus is insufficient to ionize krypton (which we verified experimentally by turning off the UV pulses)—its presence in the trace suggests an additional ionization channel. With the help of 3D single-active-electron simulations of the interaction of the composite $(3\omega + 1\omega)$ light field with a model Kr atom,

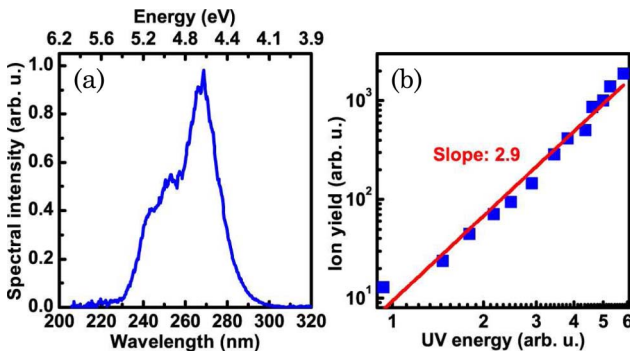


Fig. 2. (Color online) (a) Spectrum of the UV pulse and (b) Kr^+ ion yield measurements versus energy of the UV pulses.

we have identified this channel to be a $3\text{UV} + 1\text{IR}$ resonantly enhanced multiphoton ionization [21]. Because the yield of this ionization channel depends linearly on the energy of the residual NIR laser pulses, it gives rise to a linear autocorrelation trace, at the frequency of the laser, superimposed on the third-order UV trace. Owing to its linear character, it can be unambiguously subtracted from the autocorrelation trace via a numerical band-block filtering in order to facilitate its more detailed analysis. Note that despite the first-order volume autocorrelations averaging out to zero [22], the spatial confinement of the UV pulses and, therefore, of the $3\text{UV} + 1\text{IR}$ process to within a fraction of that of the NIR pulses can enable linear contributions [23].

In the first approach, the best fit to the fringe-averaged envelope is shown in Fig. 3(b) as a dashed curve, with a temporal width of $\tau_{\text{ac}} = 3.6$ fs. The duration of the UV pulses τ_{UV} can be calculated as $\tau_{\text{UV}} = \tau_{\text{ac}}/d$, where the deconvolution factor d depends on both the order of

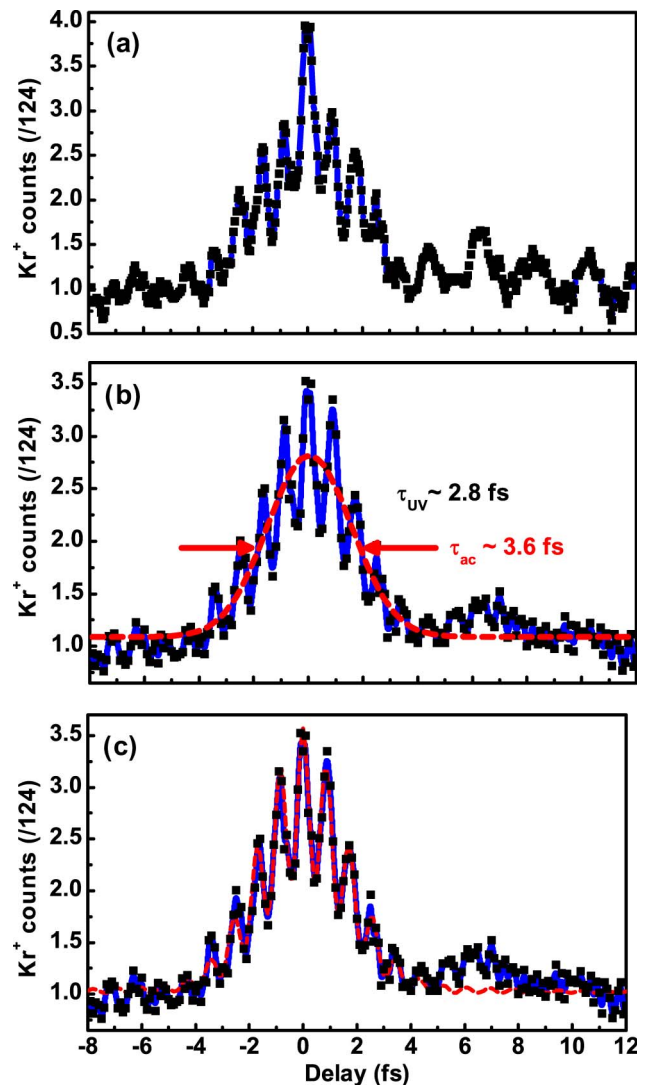


Fig. 3. (Color online) (a) Variation of the Kr^+ yield as a function of the delay between the two UV pulses (square dots; blue is guide for the eye). (b) Fringe-averaged fitting (red dashed) of the trace (blue solid) upon filtering out linear contributions of the residual laser pulses. (c) Model fitting (red dashed) of the filtered trace (blue solid).

the autocorrelation and the pulse shape. Based on the simulated third-order autocorrelation trace of the bandwidth-limited pulse, which is composed of the spectrum of Fig. 2(a), we derive $d = 1.3$. This yields an FWHM pulse duration of $\tau_{UV} \sim 2.8$ fs. The result is consistent with the ~ 2.5 fs Fourier limit that can be evaluated from the UV spectrum shown in Fig. 2(a).

In the second approach [Fig. 3(c)], we fit the filtered trace by a synthetic autocorrelation trace that we construct for a pulse with a spectrum, shown in Fig. 2(a), and a second-order spectral phase used as a fit parameter. To account for the geometric features of the all-reflective autocorrelator, we have generalized the theoretical approach introduced in [22] to a third-order nonlinearity. The synthetic trace with the highest merit of fitness to the experimental data is shown (red dashed curve) along with the filtered experimental trace in Fig. 3(c) and yields an FWHM duration of the UV pulse of 2.8 fs in good agreement with the result of our more simple analysis based on fringe-averaged autocorrelation.

Adding the demonstrated intense sub-3 fs deep-UV pulses to the toolbox of attosecond technology will advance ultrafast spectroscopy in several ways. Efficient creation of superposition states in the valence band via single-photon or few-photon excitation will allow launching of valence electron wavepackets in neutral molecules for the first time (to our knowledge). The subsequent electron wavepacket dynamics in molecular orbitals can be studied in the absence of strong NIR fields via time-resolved absorption or photoelectron spectroscopy implemented with weak attosecond probe pulses. The resolution of this time-resolved spectroscopy is limited by the duration of the excitation extending over where the number of UV photons absorbed resonantly. We expect this resolution to approach and overcome the 1 fs frontier in the foreseeable future, providing unprecedented access to a wide range of electron dynamics in the valence shell of atoms, molecules, nanoassemblies, and clusters.

We thank D. Charalambidis for fruitful discussions. We acknowledge support from Max-Planck-Gesellschaft (Max Planck Society), the Nobel Program of King Saud University, the Deutsche Forschungsgemeinschaft (DFG) Cluster of Excellence: Munich Centre for Advanced Photonics, and the training network Ultrafast Dynamics using Attosecond and XUV Free Electron Sources. E. G. acknowledges a reintegration grant from the Marie Curie European Reintegration (MERG-CT-2007-208643). R. K. acknowledges funding from the Sofja Kovalevskaja Award of the Alexander von Humboldt Foundation and an ERC Starting Grant.

References

1. M. Hentschel, R. Kienberger, C. Spielmann, G. A. Reider, N. Milosevic, T. Brabec, P. Corkum, U. Heinzmann, M. Drescher, and F. Krausz, *Nature* **414**, 509 (2001).
2. E. Goulielmakis, M. Schultze, M. Hofstetter, V. S. Yakovlev, J. Gagnon, M. Uiberacker, A. L. Aquila, E. M. Gullikson, D. T. Attwood, R. Kienberger, F. Krausz, and U. Kleineberg, *Science* **320**, 1614 (2008).
3. M. Drescher, M. Hentschel, R. Kienberger, M. Uiberacker, V. Yakovlev, A. Scrinzi, T. Westerwalbesloh, U. Kleineberg, U. Heinzmann, and F. Krausz, *Nature* **419**, 803 (2002).
4. M. F. Kling, C. Siedschlag, A. J. Verhoef, J. I. Khan, M. Schultze, T. Uphues, Y. Ni, M. Uiberacker, M. Drescher, F. Krausz, and M. J. J. Vrakking, *Science* **312**, 246 (2006).
5. F. Remacle, M. Nest, and R. D. Levine, *Phys. Rev. Lett.* **99**, 183902 (2007).
6. S. Lunnemann, A. I. Kuleff, and L. S. Cederbaum, *Chem. Phys. Lett.* **450**, 232 (2008).
7. T. Nagy and P. Simon, *Opt. Lett.* **34**, 2300 (2009).
8. P. Baum, S. Lochbrunner, and E. Riedle, *Appl. Phys. B* **79**, 1027 (2004).
9. C. G. Durfee, S. Backus, H. C. Kapteyn, and M. M. Murnane, *Opt. Lett.* **24**, 697 (1999).
10. T. Fuji, T. Suzuki, E. E. Serebryannikov, and A. Zheltikov, *Phys. Rev. A* **80** (2009).
11. S. Backus, J. Peatross, Z. Zeek, A. Rundquist, G. Taft, M. M. Murnane, and H. C. Kapteyn, *Opt. Lett.* **21**, 665 (1996).
12. N. A. Papadogiannis, G. Nersisyan, E. Goulielmakis, T. P. Rakitzis, E. Hertz, D. Charalambidis, G. D. Tsakiris, and K. Witte, *Opt. Lett.* **27**, 1561 (2002).
13. K. Kosma, S. A. Trushin, W. E. Schmid, and W. Fuss, *Opt. Lett.* **33**, 723 (2008).
14. U. Graf, M. Fiess, M. Schultze, R. Kienberger, F. Krausz, and E. Goulielmakis, *Opt. Express* **16**, 18956 (2008).
15. E. Constant, E. Mevel, A. Zair, V. Bagnoud, and F. Salin, *J. Phys. IV* **11**, Pr2-537 (2001).
16. P. Tzallas, D. Charalambidis, N. A. Papadogiannis, K. Witte, and G. D. Tsakiris, *Nature* **426**, 267 (2003).
17. Y. Nomura, R. Horlein, P. Tzallas, B. Dromey, S. Rykovanov, Z. Major, J. Osterhoff, S. Karsch, L. Veisz, M. Zepf, D. Charalambidis, F. Krausz, and G. D. Tsakiris, *Nature Phys.* **5**, 124 (2009).
18. T. Sekikawa, A. Kosuge, T. Kanai, and S. Watanabe, *Nature* **432**, 605 (2004).
19. A. L. Cavalieri, E. Goulielmakis, B. Horvath, W. Helml, M. Schultze, M. Fiess, V. Pervak, L. Veisz, V. S. Yakovlev, M. Uiberacker, A. Apolonski, F. Krausz, and R. Kienberger, *New J. Phys.* **9**, 242 (2007).
20. D. Descamps, L. Roos, C. Delfin, A. L'Huillier, and C. G. Wahlstrom, *Phys. Rev. A* **64** 031404 (2001).
21. M. D. Perry and O. L. Landen, *Phys. Rev. A* **38**, 2815 (1988).
22. H. Mashiko, A. Suda, and K. Midorikawa, *Appl. Phys. B* **87**, 221 (2007).
23. O. Faucher, P. Tzallas, E. P. Benis, J. Kruse, A. P. Conde, C. Kalpouzos, and D. Charalambidis, *Appl. Phys. B* **97**, 505 (2009).